Published July 1, 1987

Two Distinct Attachment Sites for Vimentin along the Plasma Membrane and the Nuclear Envelope in Avian Erythrocytes: A Basis for a Vectorial Assembly of Intermediate Filaments

Spyros D. Georgatos and Günter Blobel

Laboratory of Cell Biology, Howard Hughes Medical Institute, The Rockefeller University, New York, New York 10021

Abstract. In vitro binding studies with isolated bovine lens vimentin and avian erythrocyte membranes reveal the existence of two functionally distinct sets of intermediate filament attachment sites. One population of such receptors is located along the nuclear envelope and comprises polypeptides recognizing the carboxy-terminal tail domain of vimentin. Vimentin associates with these nuclear surface receptors in a cooperative manner and forms extensive 10-nm filaments in a concentration-dependent fashion. Conversely, the plasma membrane contains binding sites that interact in a noncooperative, saturable fashion with vimentin, recognizing its amino-terminal head domain. The functional dichotomy of the vimentin-binding sites under in vitro conditions may reflect a vectorial assembly process whereby 10-nm filaments, although structurally apolar, acquire polar features brought about by the differential attachment to specific receptors arranged along the plasma membrane and the nuclear envelope.

Due to the complexity of the subplasmalemmal region of eukaryotic cells, where numerous cytoskeletal elements converge or anastomose, only a few model systems have been used so far for studying the association of filaments with membranes (lens, erythrocytes, etc.) (14, 27). Within these boundaries we have recently analyzed the molecular interactions of the intermediate filament (IF)[1] subunit vimentin with the plasma membrane using the anucleate human erythrocyte as a model system and using several quantitative criteria to assess the specificities involved. In this manner, the polypeptide ankyrin (or band 2.1), a major component of the so-called membrane skeleton, was characterized as a high-affinity vimentin acceptor (11). The binding was found to be highly site-specific. The associating regions comprised the amino-terminal head domain of vimentin and a segment on ankyrin adjacent to, but distinct from, the spectrin-binding site, which is also contained in the same 55–60-kD domain of this molecule (12, 13; Weaver, D., and S. Georgatos, manuscript in preparation). In vitro polymerization studies revealed that the binding of isolated ankyrin to vimentin oligomers prevents the formation of IFs, which are otherwise assembled from purified subunits under similar solution conditions (12). The latter observation, together with other data that show a dependence of the binding on the concentration of polymer ends, as well as its saturable and noncooperative character, led us to the conclusion that the plasma membrane provides exclusively termination attachment sites for IF and that the putative centers from which IF assembly is initiated should reside in a different cellular domain. The nuclear envelope seemed a reasonable candidate for such a nucleation function. We therefore sought to develop an in vitro assay whereby the binding of purified IF subunits to plasma and nuclear membranes of the same cell could be accurately measured and meaningfully compared. Here, the results of this effort are reported, showing that vimentin filaments can only be assembled from nuclear envelope–associated sites, which are distinct from their plasma membrane counterparts in function and specificity.

1. *Abbreviation used in this paper*: IF, intermediate filament.

Materials and Methods

Nuclear Envelope Isolation

70–80 ml of blood was collected from the wing veins of turkeys into heparinized tubes. The blood was briefly centrifuged to separate the plasma from the formed elements (~1,000 *g*, 10 min, 4°C). The "buffy coat" (containing white blood cells and platelets) was removed by aspiration. The remaining red cells were washed with a total of 300 ml of PBS (150 mM NaCl, 10 mM $NaPO_4$, pH 7.4) at 0°C. To osmotically disrupt the erythrocytes, 360 ml of lysis buffer (5 mM $NaPO_4$, 2 mM $MgCl_2$, 2 mM β-mercaptoethanol, 1 mM phenylmethylsulfonyl fluoride (PMSF), pH 7.6) was added to ~25 ml of packed cells. The suspension was stirred on ice for 15 min.

The resulting nucleated erythrocyte ghosts were harvested by centrifugation (16,000 *g*, 1 min, 4°C). The leukocyte button was discarded, and the ghosts were resuspended at a hematocrit of 10% in fresh lysis buffer. 10-ml aliquots of this suspension were sonicated (Sonifier Cell Disruptor 100, setting of 3, meter reading 50–60; Branson Sonic Power Co., Danbury, CT) at 0°C for 15–20 s in a conical corex tube. Enucleation was checked by phase-contrast microscopy. The preparation was centrifuged (~1,500 *g*, 5 min, 4°C) to separate the nuclei from plasma membranes. The upper two-thirds of the supernatant was collected and kept for plasma membrane isolation. The pellet (nuclei) was resuspended in 15 ml of lysis buffer and passed

Published July 1, 1987

three times through a 23-gauge needle, bent in a Z shape, to remove contaminants and debris adhering to the nuclei. The nuclear suspension was centrifuged as above and the pellet was washed once with 25 ml of lysis buffer. Finally, the washed nuclei were resuspended in 10 ml of the same media and divided into two 5-ml aliquots.

To each aliquot, 250 μl of DNase I (2 mg/ml in PBS-1 mM PMSF), 25 μl of 1 M $MgCl_2$, and 500 μl of 10× PBS were added sequentially under vortexing. After an incubation (15 min, room temperature), the preparation was centrifuged through a cushion of 10% sucrose (5 ml in PBS at 12,000 *g* for 10 min and at 4°C). Digestion with the nuclease was repeated once more in exactly the same manner. The pellet was resuspended in 35 ml of PBS-1 mM PMSF and centrifuged as above yielding nuclear envelopes. Part of the preparation was kept in PBS-2 mM $MgCl_2$, 0.5 mM PMSF pH 7.6 at 0°C. The rest was processed further (see below).

Plasma Membrane Isolation

The first postnuclear supernate was passed three times through a 23-gauge syringe needle (as above) and centrifuged (2,000 *g*, 15 min, 4°C) to pellet any remaining nuclei. The upper two-thirds of the supernatant were aspirated with a syringe and sedimented at 16,000 *g* for 30 s at 4°C. The pellet was discarded, while the supernatant was further centrifuged (16,000 *g*, 30 min, 4°C). The top, whitish layer was gently detached from the rest of the redish pellet by turning the tube and was resuspended in 35 ml of 5 mM $NaPO_4$, 1 mM EDTA, 2 mM 2-mercaptoethanol, 0.5 mM PMSF, pH 7.6. The membranes were re-pelleted yielding plasma membranes. Part of the preparation was kept in 5 mM $NaPO_4$, 0.5 mM PMSF, pH 7.6 at 0°C. The rest was processed further (see below).

Extraction of Endogenous Vimentin from Plasma and Nuclear Membranes

Nuclear envelopes or plasma membranes (see above) were resuspended in 30–40 vol of 5–10 mM $NaPO_4$, 0.5 mM PMSF, pH 7.6 or alternatively, in glass-distilled water. The preparations were vigorously vortexed for 10–15 s and then centrifuged at 16,000 *g* for 30 min at 4°C. The pellets were resuspended in the same media and stirred overnight (12–18 h) at 0°C. After pelleting as above, the membranes were washed once in PBS (nuclear envelopes) or 5 mM $NaPO_4$ (plasma membranes) and finally resuspended in PBS-2 mM $MgCl_2$–0.5 mM PMSF pH 7.6 or 5 mM $NaPO_4$, 0.5 mM PMSF pH 7.6. They were kept on ice for a maximum of 5 d.

Purification of Vimentin

Vimentin was purified from calf lens essentially as previously described (12) with the following modifications: (*a*) The $(NH_4)_2SO_4$ precipitation step was eliminated from the protocol, and (*b*) ion-exchange chromatography was carried out with 10 mM $NaPO_4$, 1 mM EDTA, 5 mM β-mercaptoethanol, 0.2 mM PMSF, and 8 M urea, pH 7.4 as a basal buffer and at room temperature. Elution was achieved with a 0–200 mM NaCl gradient.

Iodination of Vimentin

Purified vimentin was iodinated by the ^{125}I-Bolton–Hunter reagent (2,000 Ci/mmol) as specified previously (12).

Digestion of Membranes with Proteolytic Enzymes

Plasma membranes or nuclear envelopes were washed with PBS and then incubated with trypsin (enzyme/protein ratio 1:80) for 20 min at 0°C. The reaction was stopped by adding PMSF (to 1.3 mM). The digested membranes were extensively washed with PBS-1 mM PMSF and used for assays. No protease activity was detectable in these preparations upon coincubation with ^{125}I-vimentin.

Digestion of Nuclear Envelopes with Nucleases

Vimentin-depleted nuclear envelopes (2.5 mg/ml) were digested at room temperature with a mixture of DNase I and RNase A each at a concentration of 0.15 mg/ml for 20 min. The envelopes were pelleted (12,000 *g*, 30 min) and washed three times with PBS, 2 mM $MgCl_2$, 0.5 mM PMSF pH 7.6 before assaying.

Chymotryptic Cleavage of Vimentin

^{125}I-Vimentin was dialyzed against 5 mM $NaPO_4$ pH 7.6 (4°C) and then digested with α-chymotrypsin exactly as described by Geisler et al. (9). Digestion was stopped by PMSF (to 1.3 mM), cooling on ice, and adjustment of salt to isotonic by the addition of 10× PBS. The digests remained stable for at least 1 wk on ice.

Antibodies

Immunoblotting data presented in this paper were produced by an anti-vimentin antibody (polyclonal) recognizing both avian and mammalian vimentin (provided by Dr. E. Wang, The Rockefeller University). The characterization of the anti-ankyrin antibody has been described previously (11).

Binding Assays

^{125}I-Vimentin (at a specific activity of 200,000 cpm/μg) and in 2 mM $NaPO_4$, 0.1 mM PMSF pH 7.6 was combined with 40 μg of plasma membranes or 70 μg of nuclear envelopes. The salt was adjusted to 150 mM NaCl, 10 mM $NaPO_4$, 0.3 mM $MgCl_2$, 0.1 mM PMSF pH 7.6 and the final volume to 120–150 μl. BSA was included in the assay mixture (at a concentration of 0.1 mg/ml) to prevent nonspecific adsorption to the plastic. Incubations were for 50 min (nuclear envelopes) and for 90 min (plasma membranes). After that, the reaction mixtures were transferred to 400-μl hard polyethylene tubes over a 120-μl cushion of isotonic (4%) sucrose with an air bubble in-between. Bound ^{125}I-vimentin was separated from nonbound by sedimentation at 12,000 *g* for 28 min at 4°C. The tubes were immediately frozen in liquid N_2 and dissected with a razor blade. The pellet-containing tips and the rest of the tube were then counted for radioactivity. Prestandardization of the pelleting system showed that 99.3% of the membranes are pelleted under these conditions, while <0.3% of the ^{125}I-vimentin is sedimented in the absence of membranes. For each binding curve individual points were averages of at least four independent observations. The variation was always <10%.

Immunoblotting

Proteins, separated by SDS-PAGE, were electrophoretically transferred to nitrocellulose sheets. The blots were processed exactly as described by Granger and Lazarides (16) with 0.1% gelatin as a blocking and carrier protein. Antibody dilutions were 1:100 for anti-ankyrin and 1:200 for anti-vimentin. *Staphylococcus aureus* protein A-^{125}I was applied to 0.3 μCi/ml at a specific activity of 10 μCi/μg.

Electrophoresis

Electrophoresis was according to Laemmli (21).

Protein Determinations

Protein concentrations were estimated according to Lowry (23) with BSA as a standard. The protein content of individual gel bands (that had been stained by Coomassie Brilliant Blue) was estimated after an overnight extraction with pyridine (6). BSA was used as a standard.

DNA Determinations

The DNA content of the membranes was estimated according to Ceriotti (5) using salmon sperm DNA as a standard.

Electron Microscopy

Samples were applied to formwar-coated, glow-discharged, 300-mesh grids for 1 min at room temperature. Excess liquid was removed by capillary action, and the grids were washed with a few drops of isotonic NaCl buffer. Samples were then negatively stained with 1% uranyl acetate (15–50 s, room temperature), air-dried, and visualized in a Philips 300 electron microscope operated at 80 kV.

Results

Assay System

To compare the binding of vimentin with nuclear versus plasma membranes, the avian erythrocyte was chosen as a model system. This cell provides an excellent source of nu-

Published July 1, 1987

clear and plasma membranes, which could be isolated free of cytoplasmic contaminants. In its mature form the avian red cell contains a limited number of cytoplasmic organelles (4). More importantly, its cytoskeletal elements are well segregated: the microtubules are localized beneath the plasma membrane as a marginal disc, all actin microfilaments are sequestered in the subplasmalemmal membrane skeleton, while the IFs extend from the nuclear periphery to the plasma membrane, away from the marginal disc (14, 15, 22, 36).

The method of Beam et al. (2) was used to obtain nuclear envelope and plasma membrane fractions. This technique involves controlled sonication of osmotically disrupted red cells (ghosts) in low salt and Mg^{++}-containing media. Furthermore, a combination of established methods (hydraulic shearing through bent syringe needles and differential centrifugation) was used to effectively separate the membranes from cross-contaminants. For the preparation of nuclear envelopes, isolated nuclei were routinely treated with DNase I, which digested the bulk of the DNA. The SDS-PAGE profiles depicted in Fig. 1 *a* show the polypeptide composition of the two membrane fractions. The plasma membrane fraction contained the characteristic polypeptides ankyrin, spectrin, band 3, actin, etc. and was free of histones or lamins. Conversely, the nuclear envelope preparation included the lamins and some residual histones. The nuclear lamina of birds comprises basically two proteins corresponding to mammalian lamin A and B (20, 30), as indicated by two-dimensional peptide mapping (data not shown). A third band, with a molecular mass similar to rat liver lamin C, is in fact not a lamin but possesses features of an integral membrane constituent (see companion paper). Small quantities of residual spectrin contaminated the nuclear fractions, as reported by Jackson (18). This material could not be removed by density gradient sedimentation or washings. However, cross-contamination with ankyrin (if any) was minimal, since none of it could be detected by immunoblotting (Fig. 4 *a*).

Most of the endogenous IFs were removed from the membrane preparations by severing the filaments during sonication. Nevertheless, the nuclear envelopes contained ~4 μg of vimentin per mg of total protein and the plasma membranes ~0.5 μg of vimentin per mg of total protein (as estimated by dye extraction of Coomassie Blue–stained gels)

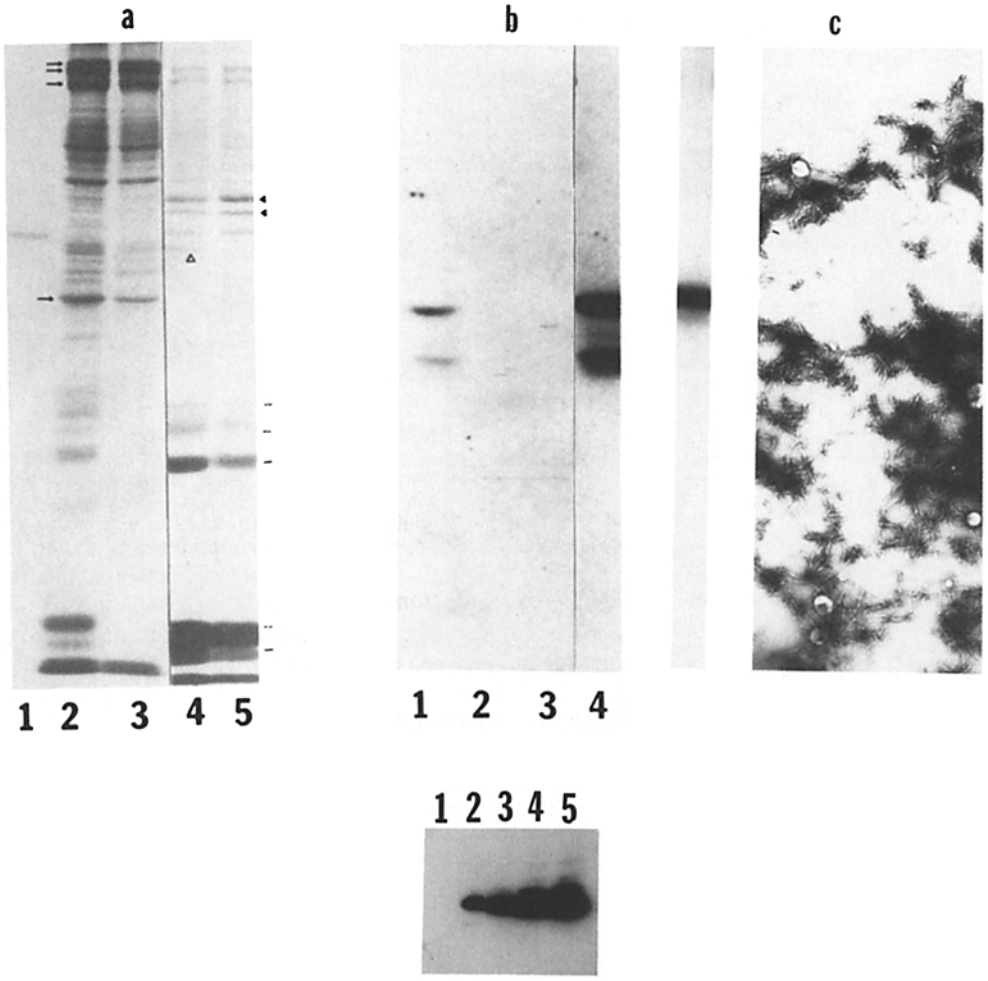

Figure 1. (*a*) Fractionation of turkey erythrocyte membranes. SDS-PAGE profiles. Lane *1*, a sample of purified lens vimentin shown here as a reference marker; lane *2*, plasma membranes before low-salt (phosphate) extraction; lane *3*, plasma membranes after extraction; lane *4*, nuclear envelopes before extraction; lane *5*, nuclear envelopes after extraction (10% acrylamide gel stained with Coomassie Blue). Small arrows show (from *top* to *bottom*) the positions of ankyrin, α-spectrin, β-spectrin, and actin. Dashes point to the histones, and filled arrowheads to the avian lamin A (upper band) and lamin B (lower band). Open arrowhead indicates the endogenous avian RBC vimentin. (*b*) Removal of endogenous vimentin from turkey membranes as detected by immunoblotting with anti–vimentin antibodies (an autoradiogram is shown). Lane *1*, whole turkey RBC ghosts; lane *2*, phosphate-extracted plasma membranes; lane *3*, phosphate-extracted nuclear envelopes; lane *4*, combined phosphate extracts (10 times concentrated). The lower band (~40 kD) represents a breakdown product of vimentin, usually detected upon prolonged handling of the preparation. The lower panel shows immunoblotting data of phosphate-extracted nuclear envelopes (lane *1*, 70 μg of protein) and 50 (lane *2*), 100 (lane *3*), 200 (lane *4*), and 400 ng (lane *5*) of purified vimentin using an anti–vimentin antibody. (*c*) Status of the lens vimentin used in the study. (*Left*) An autoradiogram of purified ^{125}I-vimentin. (*Right*) An image of 10-nm filaments reconstituted from purified vimentin as seen after negative staining with 1% uranyl acetate (vimentin conc. ≅600 μg/ml). For details see Materials and Methods.

Published July 1, 1987

(6). This residual material could be readily extracted by washing both membrane fractions in low ionic strength phosphate buffers without divalent cations. As shown in Fig. 1 *b*, no endogenous vimentin can be detected by immunoblotting assays with an anti-vimentin antibody that would readily detect nanogram amounts of the corresponding antigen. The specific effect of phosphate ions on the solubility of IFs has been noted by others (1, 28, 37).

To probe the binding of IF subunits to the erythrocyte membranes, we used bovine lens vimentin (see Materials and Methods). The mammalian form of vimentin is structurally almost identical to the avian vimentin (26, 35, 38) and can be easily purified in mass quantities and in a polymerization-competent form (Fig. 1 *c*). Moreover, its polymerization and sedimentation properties have been explored in our previous in vitro studies (12), which indicated that, up to 100 μg/ml, this material exists predominantly as a soluble species (~85%) with a sedimentation coefficient of 6.75. At higher concentrations the amount of soluble vimentin decreases. Recent studies have established that the soluble vimentin form represents a tetramer (31). Such an interpretation has been confirmed in a series of cross-linking experiments we have done using the agent dimethyl suberimidate (Georgatos, S., unpublished results).

Vimentin Attachment Sites at the Plasma Membrane

When ^{125}I-labeled vimentin was incubated with erythrocyte plasma membranes, a hyperbolic binding isotherm was obtained (Fig. 2 *C*). The shape of the curve indicated a saturable association. When equivalent amounts of washed, intact erythrocytes were substituted for the plasma membranes, much less binding was observed, strongly suggesting that the vimentin–membrane interaction observed in vitro was restricted to the cytoplasmic face of the membrane and therefore was physiologically meaningful. The proteinaceous nature of the plasma membrane–binding sites was demonstrated by showing that trypsinized membranes were unable to bind vimentin (Fig. 2 *C*).

Electron microscopic visualization of plasma membranes reconstituted with purified vimentin (at 400 μg/ml) revealed no apparent filament formation onto the membranes (Fig. 3 *c*), a finding compatible with the saturable character of the binding isotherm presented above. By Scatchard plotting of the data (Fig. 2 *D*) (29), two vimentin binding site classes were evident: a high-affinity site (K_a ~8×10^6 M^{-1}) and a low-affinity site (K_a ~6.2×10^5 M^{-1}). By Hill analysis (17), a coefficient of 1.02 was estimated, indicating the absence of cooperativity. Similar studies with the human erythrocyte membrane (11) had yielded only a single vimentin-binding site.

Antibodies raised against human erythrocyte ankyrin have the potential of completely blocking the binding of vimentin to human inside-out RBC vesicles (11). The same reagents could suppress the binding of ^{125}I-vimentin to turkey RBC plasma membranes by 40% (Fig. 4 *b*). These results specifically implicate avian ankyrin in the binding process. The occurrence of an alternative vimentin-binding site (as indicated by the Scatchard plot) or some known differences between avian and human ankyrin (expressed in its M_r, or in solubility properties) (2, 24) may account for the difference in the neutralizing effect of anti-ankyrin observed in the avian membranes.

Vimentin Attachment Sites at the Nuclear Envelope

Assaying of the binding of ^{125}I-vimentin to the nuclear envelopes revealed several unique features. The isotherm in this case possessed an initial sigmoidal leg, indicating the occurrence of positive cooperativity during the binding, a pseudoplateau region and, finally, a linear ascending segment at higher concentrations of the radiolabeled ligand (Fig. 2 *A*). These characteristics of the curve suggested an initial trend towards saturation followed by a clearly nonsaturable binding.

To investigate the origin and the physical meaning of the unsaturable component of the binding, various assay samples were examined by electron microscopy. When nuclear envelopes depleted of endogenous vimentin were analyzed, nuclear ghost-like structures were observed (Fig. 3, *a* and *b*). These membranes lacked any 10-nm filaments, as expected from the immunoblotting data shown previously (Fig. 1 *b*). However, upon addition of 150 μg/ml of vimentin, short 10-nm rods were seen to decorate the surfaces of the envelopes (Fig. 3 *d*, *inset*). At higher magnification the rods consisted of thinner 2–3-nm fibrils (Fig. 3 *d*, *arrowheads*). Similar unraveled filament morphologies have been noticed in keratin IF by other investigators and are believed to reflect the inherent protofibrillar substructure of assembled IF units (1).

When more vimentin (200 μg/ml) was added to the nuclear envelopes, an increase of the filament length was noticed (Fig. 3 *e*). Finally, upon reconstitution with 400 μg/ml of vimentin, extended IF arrays were formed (Fig. 3, *f* and *g*). Thus, the nuclear envelopes were able to initiate the formation of 10-nm filaments, whereas the plasma membranes were not.

Scatchard plotting of the binding data (Fig. 2 *B*) generated a convex curve with a maximum at ~80 μg of ^{125}I-vimentin bound per mg of envelope protein. This configuration of the plot is a hallmark of positive cooperativity that was also deduced by Hill analysis (Hill coefficient ~2.00). The binding was salt- and time-dependent. Equilibration was reached after ~50 min at room temperature (24°C, Fig. 5 *a*). At low salt (below 10 mM), only negligible amounts of vimentin associated with the nuclear envelopes, while a maximum binding was noted at 80–130 mM of NaCl (Fig. 5 *b*).

The proteinaceous nature of the vimentin-binding sites, as well as the specificity of the process, was demonstrated by showing that trypsinized nuclear envelopes cannot bind the radioactive tracer (Fig. 2 *A*). Digestion with nucleases (Table I) or anti-ankyrin antibodies (see companion article) did not affect the binding of vimentin to nuclear envelopes. After heat treatment (65°C, 2 min) the binding of ^{125}I-vimentin to nuclear envelopes was basically unchanged, while the binding to the plasma membranes was significantly lowered but not abolished (Table I). Finally, acetic acid, at 0.17 M, could extract or neutralize all the vimentin-binding activity of both nuclear and plasma membranes (Table I).

Mechanism of Nuclear Attachment

There are, conceivably, two ways to explain the observed assembly of 10-nm filaments on the nuclear envelopes: Filaments may first assemble in solution and then bind as such to the nuclear surface. Alternatively, soluble oligomeric subunits might bind to the nuclear envelope and, after saturation of every available binding site, in situ polymerization

Published July 1, 1987

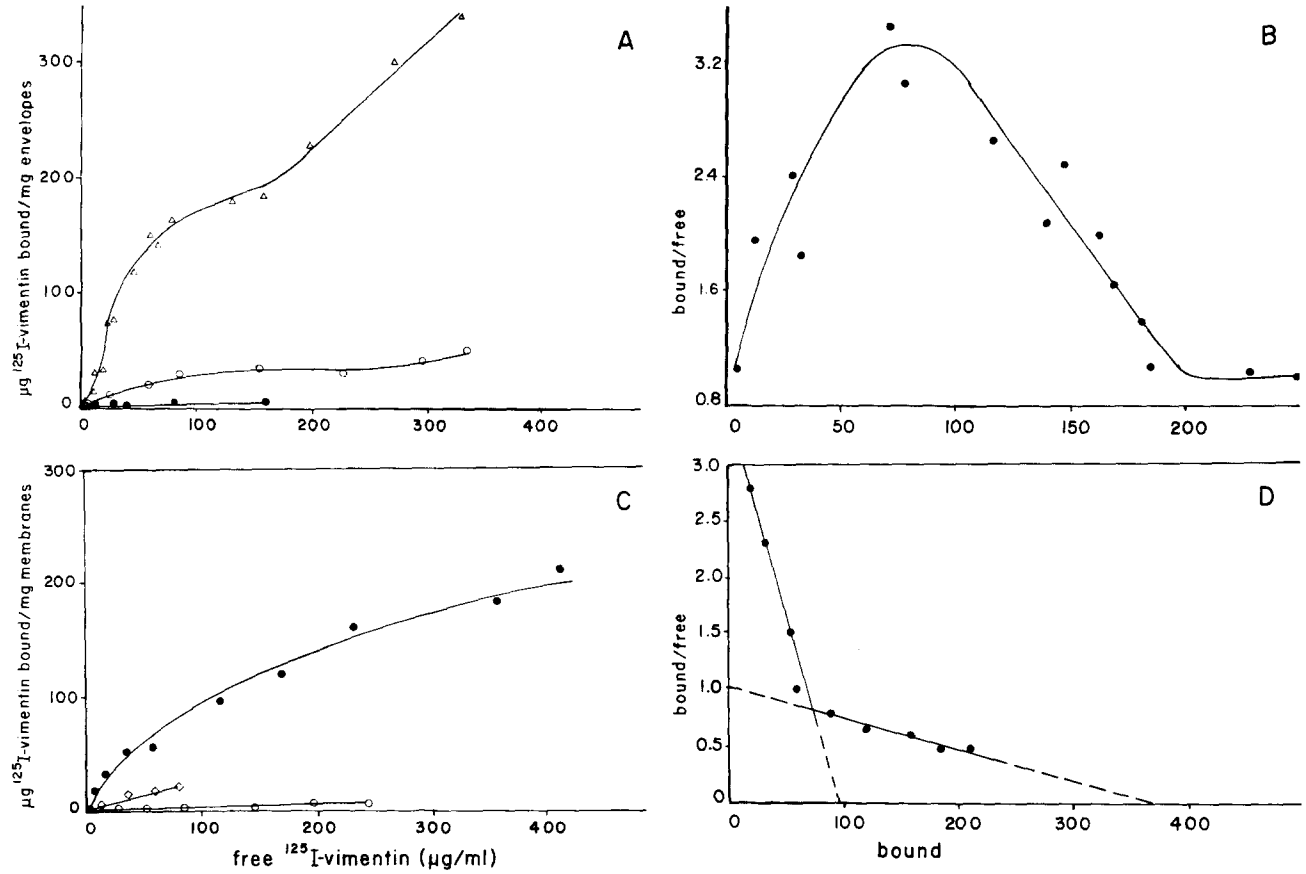

Figure 2. (*A*) Binding of ^{125}I-vimentin to phosphate-extracted nuclear membranes (△), nuclear membranes before extraction (○), and trypsinized nuclear membranes (●). (*B*) Scatchard plotting of the data shown in *A* (the last point of the isotherm is omitted). (*C*) Binding of ^{125}I-vimentin to extracted plasma membrane (●), trypsinized plasma membranes (○), or intact erythrocytes (◇). The milligram equivalent was estimated assuming 10^{-6} μg of membrane protein/cell as calculated from ghost electrophorograms. This value is similar in the order of magnitude with the one calculated for Dogde ghosts of human RBC. (*D*) Scatchard plotting of the data shown in *C*. For details see Materials and Methods.

may be accomplished by the addition of more subunits to vimentin–receptor complexes.

In principle, the data shown in Fig. 2 *A* rule out the first possibility because the change in the slope of the isotherm, after the pseudo-plateau, is not compatible with a process of binding preformed and increasingly larger polymers to the nuclear envelopes. If the latter were the case, the measurements should have yielded a straight line, starting either from the very beginning (no critical assembly concentration), or following a segment of no or very low binding (if assembly of IF does proceed when a critical subunit concentration is exceeded). Nevertheless, to better differentiate between the previously mentioned scenarios a permutation of the standard assay was used: After allowing ^{125}I-vimentin to interact with the nuclear membranes, the nonbound probe, remaining in each assay supernatant, was subjected to ultracentrifugation and separated into a soluble and a polymeric fraction. This analysis revealed that the weight concentrations of polymeric vimentin that assembled in solution did not parallel the linear increase of bound vimentin seen after raising the concentration of the total ^{125}I-vimentin (Fig. 6). Instead, the levels of this fraction remained rather constant (within a concentration range of total vimentin at which visible filaments of increasing length were detected on the surface of the envelopes). These experiments favored previous kinetic interpretations, showing that newly synthesized vimentin of chick embryo erythrocytes is rapidly incorporated into a soluble pool consisting of oligomers and then into an insoluble cytoskeletal fraction (3).

Furthermore, by assessing the binding of exogenous ^{125}I-vimentin to nuclear envelope preparations containing endogenous vimentin (Fig. 2 *A*) or intact nuclei (not shown), we discovered that these isolates exhibit both a reduced binding capacity and a lower affinity for the radiolabeled tracer. Although the capacity difference is only phenomenal and could be cancelled by considering that the vimentin-containing membranes are less enriched in authentic envelope polypeptides (three times less lamins as deduced by dye-extraction and spectrophotometry of Coomassie Blue–stained gels) and more contaminated by histones on a milligram/milligram basis, the affinity difference between vimentin-depleted and nondepleted envelopes remains substantial even after this correction (as judged by the relative slopes of the isotherms in Fig. 2 *A*). Hence, the data suggested that the primary vimentin–nuclear receptor association is stronger than the (subsequent) binding of vimentin molecules to vimentin–receptor complexes.

The same conclusion could be reached by evaluating the measurements shown in Fig. 7. In these experiments an excess of unlabeled vimentin (or BSA as a control) was used

Published July 1, 1987

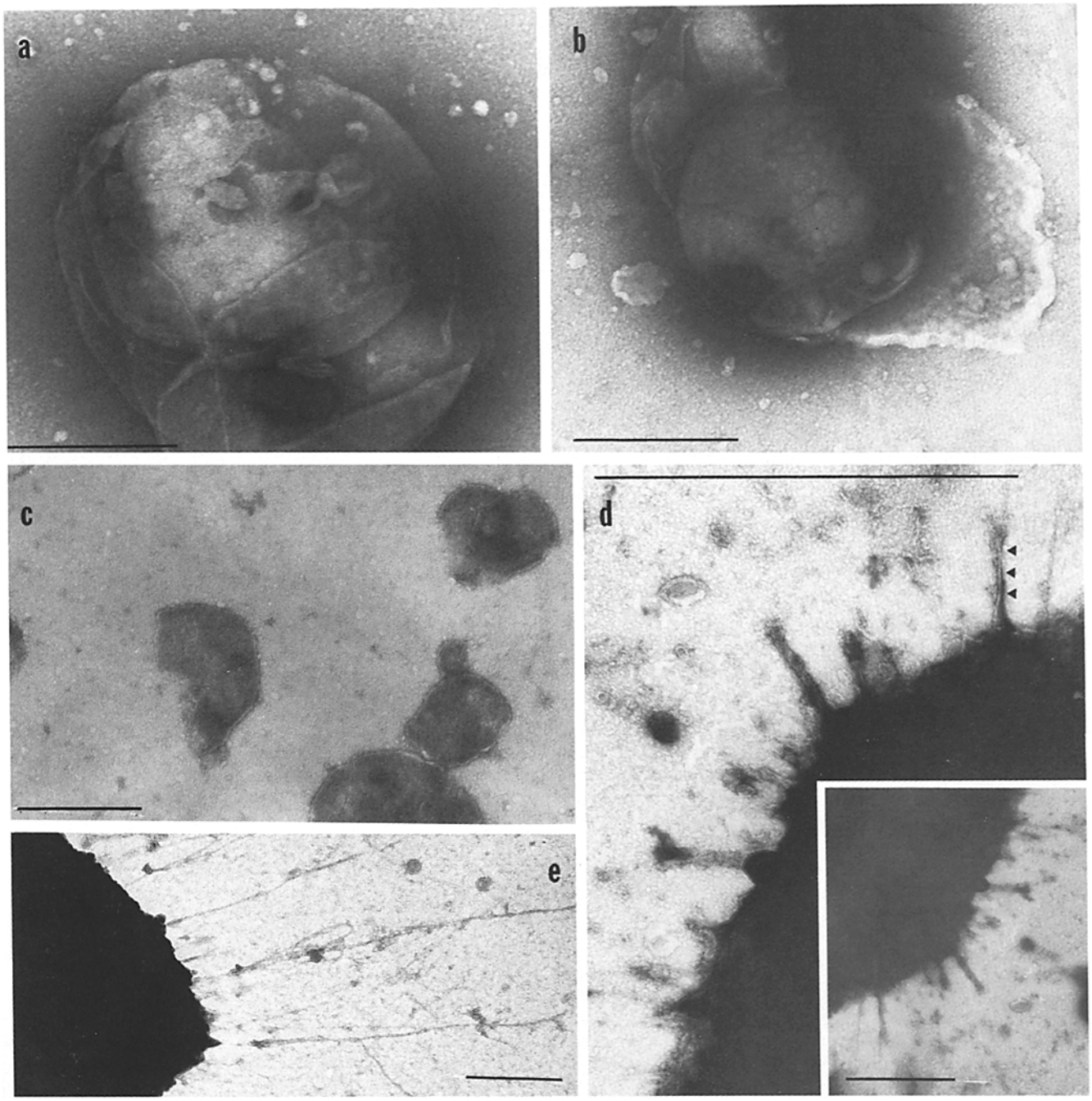

Figure 3. Electron microscopic visualization of erythrocyte membranes reconstituted with exogenous vimentin. (*a* and *b*) Vimentin-depleted nuclear envelopes. (*c*) Vimentin-depleted plasma membranes incubated with 400 μg/ml of lens vimentin. (*d*) Nuclear envelopes and 150 μg/ml of vimentin. (*e*) The same as *d* with 200 μg/ml vimentin. (*f*) The same as above with 400 μg/ml vimentin. (*g*) The same as above with 400 μg/ml vimentin. Bars, 0.5 μm.

to displace a standard amount of ^{125}I-vimentin bound to the nuclear envelopes. The apparent K_i calculated from such assays (as the vimentin concentration needed to achieve 50% displacement of the tracer) is higher than one expects on the basis of the K_d calculated from the initial segment of the isotherm shown in Fig. 2 *A*, or from the saturable binding of a vimentin peptide to the nuclear envelopes (see below). This difference can only be explained by assuming that the exchange of receptor-associated vimentin (high affinity) is coupled with the subsequent rebinding of displaced ^{125}I-vimentin to receptor–vimentin complexes (low affinity).

Site Specificity

Limited chymotryptic cleavage of IF protofilament units is known to generate basically two proteolytic fragments: a 38–40-kD middle piece, comprising the α-helical rod domain of the IF subunit molecule, and a short tail segment

Published July 1, 1987

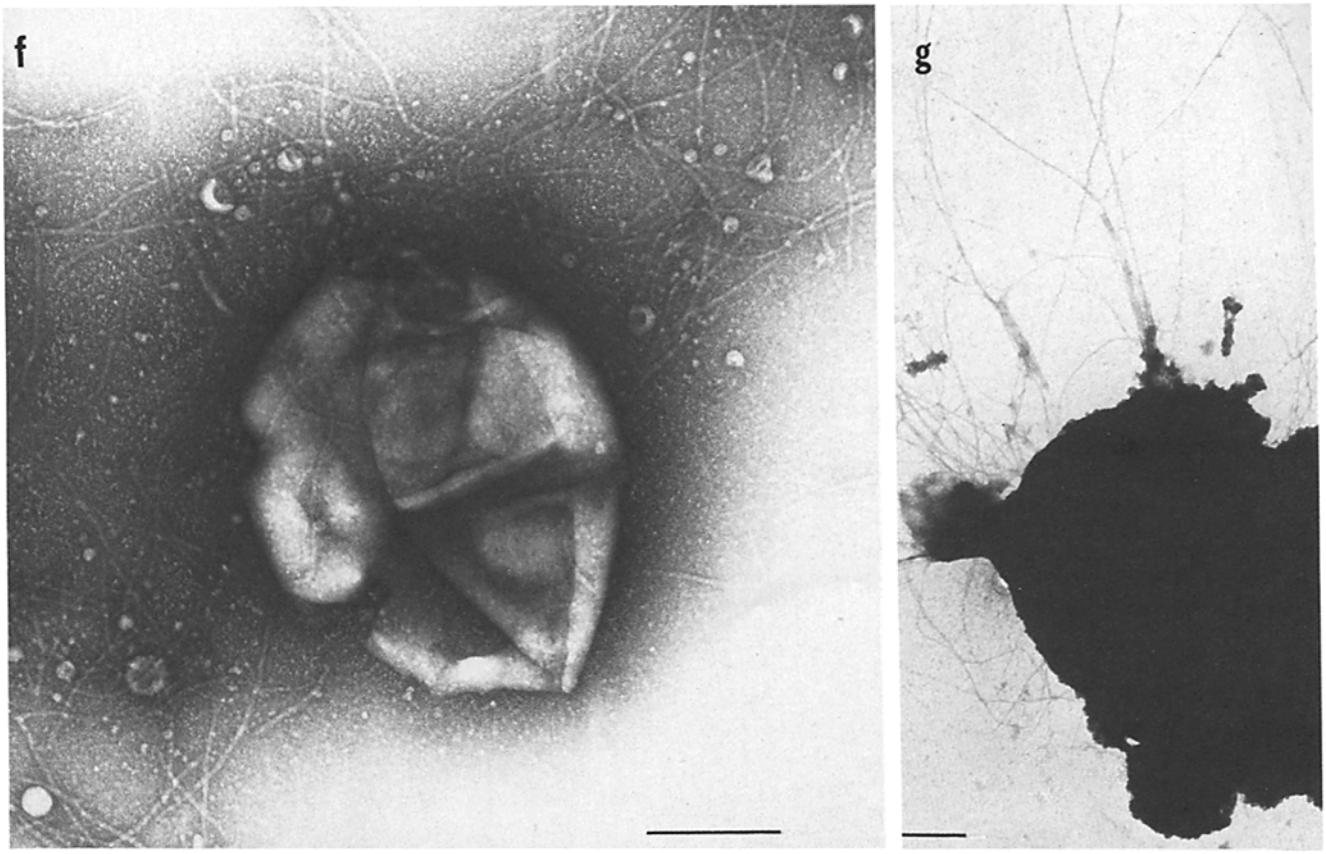

containing the carboxy terminus. At least for desmin and vimentin, the first 70–75 amino acid residues that constitute the amino-terminal head domain are largely cut into very small peptides because of the numerous, exposed (cleavage) sites occurring at this β-sheet folded part of the molecule (9, 26, 32).

Therefore, to examine the site specificity of the observed interactions, ^{125}I-vimentin was digested with chymotrypsin and the resulting peptides were combined with plasma membranes or nuclear envelopes and tested for binding. As shown in Fig. 8 *A* the 6.6-kD carboxy-terminal tail of vimentin could associate with the nuclear envelopes, while the 38-kD α-helical fragment could not. In agreement also with our previous observations (12) neither of these two domains bound to the plasma membranes, suggesting that vimentin attaches to the plasma membrane skeleton through its amino-terminal head domain. A third peptide present in the chymotryptic digest could also bind to the nuclear envelopes. This fragment may represent a cleavage intermediate containing the carboxy-terminal half of the middle domain plus the carboxy-terminal tail domain of vimentin (Fig. 8 *A*).

To quantitate the binding of the vimentin tail fragment to the nuclear envelopes, increasing amounts of the digest were incubated with the appropriate membranes and the radioactivity associated with the 6.6-kD band was measured by excising appropriate bands from the gels. An isotherm constructed from such assays is shown in Fig. 8 *B*. The binding of the fragment was saturable, as expected, because of the inability of the cleaved peptide to polymerize. The K_a of this interaction (estimated from the relative concentrations needed for 50% saturation) was in the order of 1.4×10^7 M^{-1}. Interestingly, Scatchard plotting of the data (Fig. 8 *C*)

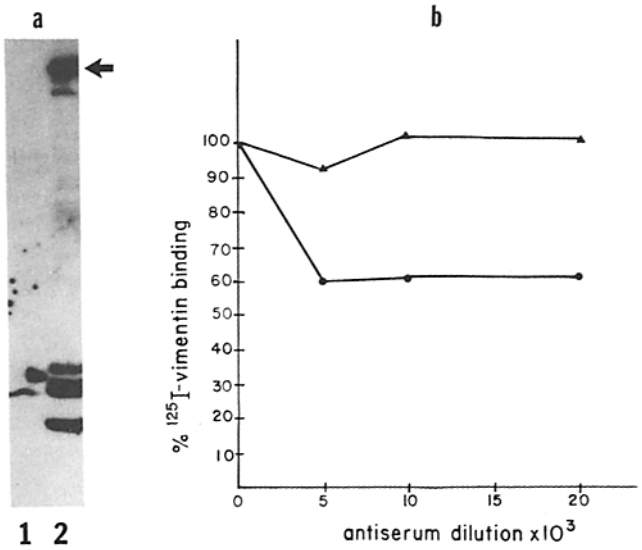

Figure 4. (*a*) Ankyrin content of red blood cell membranes as detected by immunoblotting with anti-ankyrin antibodies. Lane *1*, nuclear envelopes (extracted); lane *2*, plasma membranes (extracted). An autoradiogram is shown. For details see Materials and Methods. The position of ankyrin is indicated by an arrow. The nature of the low molecular weight products is not known but these bands most probably represent proteolytic fragments of the same polypeptide. (*b*) Effect of anti-ankyrin antibodies on the binding of ^{125}I-vimentin to (extracted) plasma membranes. The membranes (0.2 mg/ml) were preincubated for 1 h with the indicated dilutions of immune (●) or nonimmune (▲) sera. ^{125}I-Vimentin (4 μg/ml, 216,000 cpm/μg) was incubated as in the standard binding assays described in Materials and Methods. 100% binding signifies samples that received no antibodies.

Published July 1, 1987

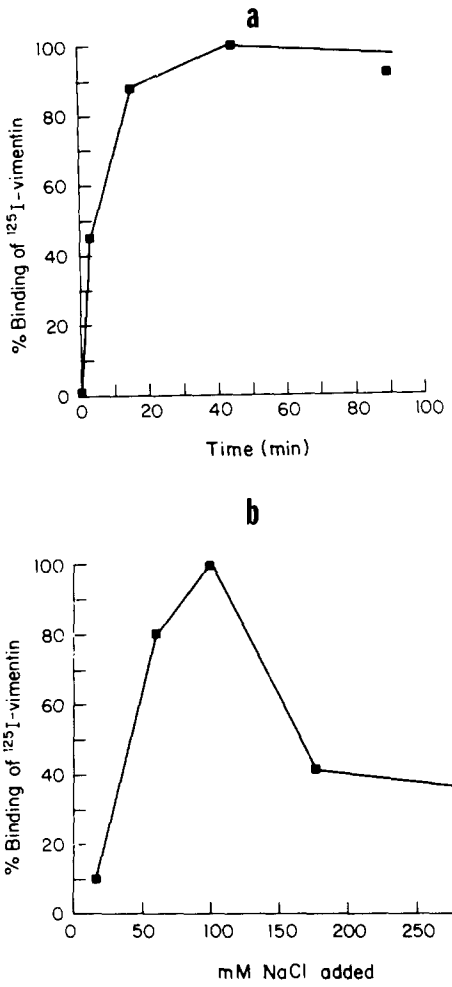

Figure 5. (*a*) Time course of the binding of ^{125}I-vimentin to nuclear envelopes. 6 μg of ^{125}I-vimentin was incubated with nuclear envelopes as specified in Materials and Methods for the time periods indicated on the abscissa. The centrifugation time was not considered for constructing the curve. (*b*) Salt dependence of the binding of ^{125}I-vimentin to nuclear envelopes. Experiments were executed as in *a* in a buffer containing 5 mM $NaPO_4$, 0.1 mM PMSF, and 2 mM $MgCl_2$ pH 7.6 plus the indicated concentrations of NaCl. The maximum binding achieved was considered 100% binding.

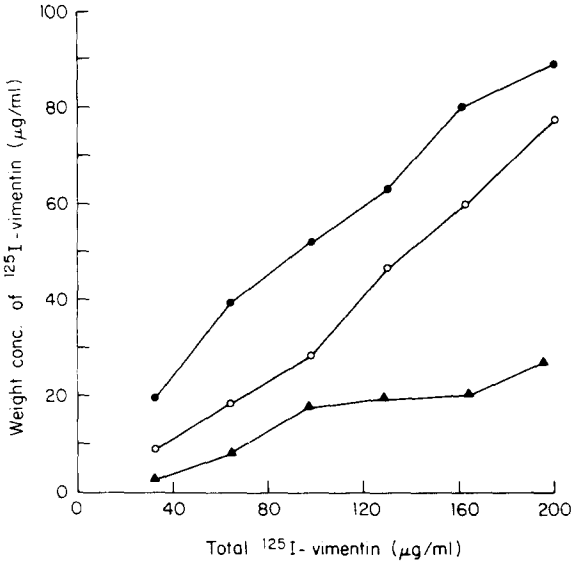

Figure 6. Centrifugational analysis of the nonbound fraction of ^{125}I-vimentin. The binding assay was executed as described in Materials and Methods and then, after the nuclear membranes were pelleted, the supernatants were collected and centrifuged at 100,000 *g* for 30 min (4°C). Radioactivity associated with the pellet or the supernatant of this centrifugation was measured and the weight concentrations of soluble (○), polymeric (▲), or bound (●) ^{125}I-vimentin were plotted as a function of the total vimentin concentration in the original assay mixture.

generated, again, a convex curve, indicating that the primary vimentin tail domain–envelope interaction was of a positive cooperative character.

Discussion

Segregated and Distinct Attachment Sites for IF

The data presented here demonstrate the occurrence of two distinct vimentin receptor systems segregated respectively into the nuclear envelope and the plasma membrane of avian erythrocytes. Quantitative binding assays, involving purified lens ^{125}I-vimentin and vimentin-depleted membrane frac-

Table I. Vimentin-binding Capacities of Membrane Preparations after Various Treatments

Membranes	Treatment	Binding of ^{125}I-vimentin	DNA/protein
		%	μg/μg
Nuclear envelopes	–	19 ± 0.1	0.44
Nuclear envelopes	Extraction with 10 mM $NaPO_4$	100	0.11
Nuclear envelopes	RNAase/DNase digestion	100 ± 0.3	0.08
Nuclear envelopes	Extracted with 0.17 M acetic acid	0.2 ± 0.0	ND
Nuclear envelopes	Extracted with 10 mM $NaPO_4$, heated at 65°C for 2 min	120 ± 0.0	ND
Plasma membranes	Extracted with distilled water	100	0.03
Plasma membranes	Extracted with 0.17 M acetic acid	7.8 ± 1.2	ND
Plasma membranes	Extracted with 10 mM $NaPO_4$, heated at 65°C for 2 min	40 ± 1.0	ND

The assays were executed as specified in Fig. 5. The extractions of the membranes were as described in Materials and Methods. ND, Not determined.

Published July 1, 1987

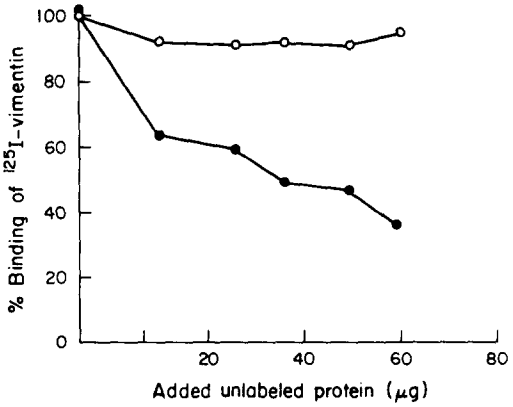

Figure 7. Displacement of bound ^{125}I-vimentin by an excess of unlabeled vimentin, (●); vimentin, (○); BSA, (control). The assays were executed as defined in Materials and Methods, with 12.7 μg of ^{125}I-vimentin (1,574 cpm/μg).

tions, indicated that vimentin interacts in a cooperative and nonsaturable fashion with the nuclear envelope, while under similar conditions, it associates saturably and noncooperatively with the plasma membrane. When analyzed by electron microscopy, the nonsaturable binding corresponds to an extensive polymerization of the envelope-associated vimentin in situ, whereas the saturable binding seems to reflect the fact that such an assembly could not take place onto a substrate like the plasma membrane. Thus, it is likely that the different quantitative parameters deduced by assessing the binding of labeled vimentin to each membrane species in vitro are genuine manifestations of two distinct attachment mechanisms.

After proteolytic cleavage of vimentin molecules (whereby their head domains are largely destroyed and their polymerization potential is lost) (19, 25, 32), their carboxy-terminal tail domains retain the ability to bind to the nuclear envelopes but not to the plasma membranes. This binding now shows saturability. Conversely, the α-helical, central domains fail to associate with either membranes. These data, in combination with previous studies (12), suggest that the site-specific recognition of the vimentin molecules by distinct and spatially separated receptors may be the principle underlying the differential mode of attachment of vimentin to the membranes.

As was previously stated (11), we have been unable to detect any interactions between vimentin and membrane phospholipids as it has been claimed by others (27, 33). Proteolyzed nuclear envelopes and plasma membranes, or acid-treated preparations, bound negligible amounts of the vimentin tracer (Table I), whereas detergent-extracted nuclear membranes were not affected (see companion paper). Therefore, we believe that the reported binding of isolated vimentin to purified phospholipids may be either irrelevant to the interactions studied here or, most likely, a reflection of an electrostatic association between the basic head domains of vimentin and some phosphate moieties occurring in proteins, lipids, and nucleic acids. However, how and where

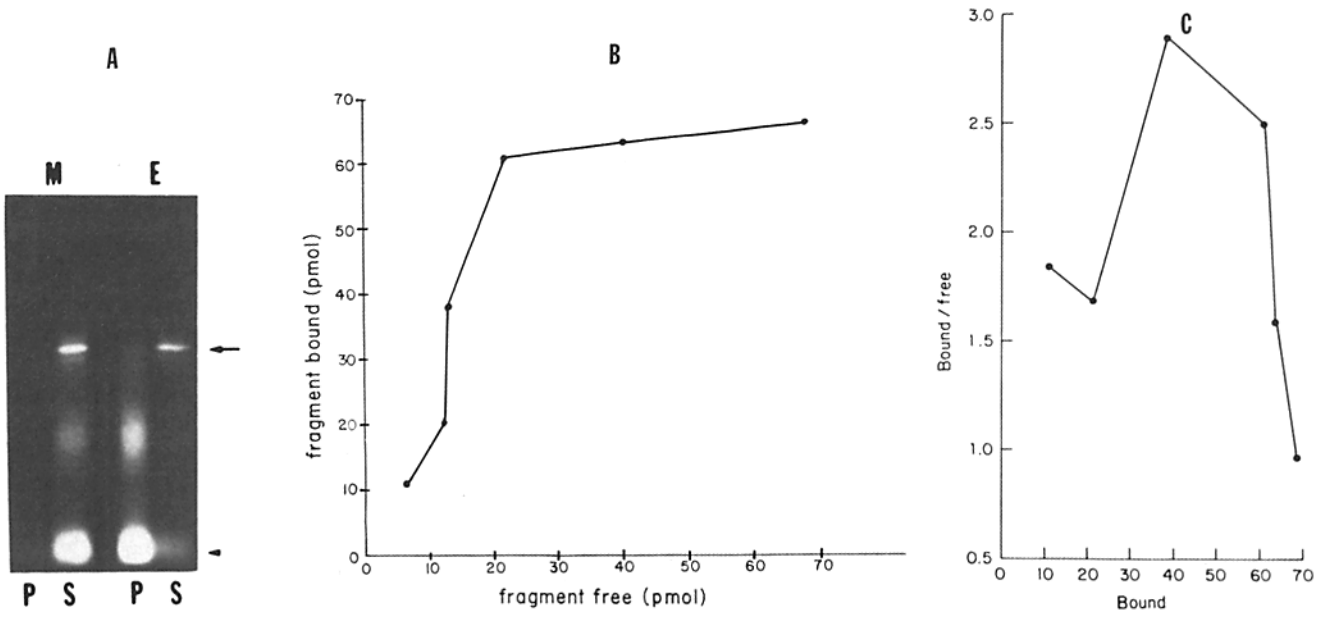

Figure 8. (*A*) Site specificity in vimentin–membrane interactions. A ^{125}I-vimentin chymotryptic digest, prepared as described (58 μg/ml vimentin, 1,700 cpm/μg) was co-incubated with plasma membranes (40 μg) or nuclear envelopes (70 μg) under standard conditions (assay volume 180 μl). The resultant pellets and supernates were subjected to electrophoresis in 15% acrylamide gels and autoradiographed. M, plasma membranes. E, nuclear envelopes. P, pellet. S, supernatant. Arrow indicates the 38-kD middle domain of vimentin and the arrowhead, its 6.6-kD domain (photographed in reverse contrast). The relatively heavier labeling of the tail piece is due to the higher accessibility of this peripheral domain to the Bolton–Hunter reagent when concentrated vimentin samples are used. Under these conditions the protein partially assembles during iodination and the coiled-coil regions are apparently protected. With more dilute preparations the labeling is proportional to the number of iodination sites occurring at the 38- and the 6.6-kD domains (more in the former and mainly Lys or His). (*B*) The binding of the 6.6-kD tailpiece to nuclear envelopes. Assays were executed as in *A* with increasing quantities of the digest. After electrophoresis the appropriate bands were excised and the radioactivity was determined by γ-counting. (*C*) The same data shown in *B* after Scatchard analysis.

Published July 1, 1987

such phosphate groups may occur (in a nonshielded state) along the membranes remains to be investigated.

The apparent heterogeneity in the vimentin receptor sites occurring at the plasma membrane of avian erythrocytes may be morphogenetically significant. Although the existence of two different receptors would not influence the direction of IF assembly (since both seem to have the same site-specificity for vimentin), the observed differences in the relative affinities for vimentin may provide a basis for establishing assymetric IF skeletons during development. Therefore, it would be interesting to fully characterize these attachment proteins and study their expression and partitioning during the various phases of erythroid development.

Vectorial Assembly

The above findings support previous morphological observations, indicating that the assembly of 10-nm filaments may occur vectorially, that is, from the nucleus towards the cell surface. As early as 1971, Franke, studying the structural associations of cytoplasmic filaments with the nuclear envelope, postulated that "the formation of such tubules and filaments is nucleated at cytomembraneous surfaces" (7). Later, Granger and Lazarides (14) noticed that chick embryonic erythrocytes possessed relatively few vimentin filaments that were associated with the nucleus but, in general, did not reach the cellular periphery. In contrast, more developed red cell forms contained numerous filaments, extending from the nuclear periphery to the plasma membrane. This suggests that 10-nm filaments may grow unidirectionally. In addition, Wang (34) reported that vimentin fibers could be assembled from intact nuclei of tissue culture cells after an incubation with purified vimentin. Therefore, it seems reasonable to infer that the initiation of IF assembly may occur in the neighborhood of the nuclear envelope.

Although a vectorial assembly route explains better the data obtained by binding studies, it does not necessarily imply the existence of two separate receptor systems with distinct site specificities. Indeed, a preferential IF assembly from the nucleus would be theoretically possible if the receptor concentrations were vastly greater at the nuclear envelope than in the plasma membrane, even if the binding sites were structurally identical in both cases. Alternatively, the receptors could have been structurally different, but functionally similar, recognizing the same vimentin domain, albeit to a different degree (different affinities). The latter possibility is an attractive one since current models for IF organization favor a structural apolarity of these assemblies. That the two dimeric pairs in each protofilament assume an anti-parallel orientation could be thought to result in linear polymers with identical ends (8, 10). Hence, it is conceivable that the membrane-bound vimentin receptors could recognize more or less the same molecular features on the polymer ends.

Our present data argue against these possibilities as clear-cut differences could be detected, not only in the capacities and affinities of the vimentin–membrane interactions, but also in the site specificities involved and the structural characteristics of the vimentin receptors (see companion article). Knowing that, one is allowed to reverse the question: Do native IFs, inside eukaryotic cells, show the same structural apolarity with the in vitro reconstituted assemblies, or differ from them in a fundamental manner?

A Model for a Receptor-modulated Assembly of IFs

Newly made vimentin subunits inside eukaryotic cells, immediately after biosynthesis, would conceivably face one of the following fates: they would either polymerize spontaneously forming free-floating cytoplasmic filaments, or they would bind as lower oligomers (i.e., tetramers, see reference 31) to membrane-associated receptors. Naturally, such a choice of binding will depend on the relative affinities involved. The first possibility is not favored by data accumulated from in vitro studies, since vimentin–vimentin associations seem weaker than nuclear envelope–vimentin interactions (this report). Conversely, vimentin–plasma membrane interactions appear to be of the same order of magnitude as the vimentin–vimentin self-association that leads to IF elongation (11, 12, and this report). Thus, one could predict that, at first, most of the newly synthesized material would be sequestered around the nucleus. Based on the cooperative binding of the vimentin tail peptide to its nuclear receptor, it is reasonable to assume also that a primary nucleus of IFs may be assembled in situ onto the nuclear envelope. Then, a gradient of affinities as described above, i.e., vimentin–vimentin binding weaker than vimentin binding to vimentin–nuclear receptor complexes and this weaker than vimentin–nuclear receptor binding, may dictate a vectorial assembly of IF units towards the cell surface.

Elongation of such units could be subsequently achieved when a certain subunit concentration value is exceeded in the cytoplasm and plasma membrane anchorage may occur as the filaments increase in length. Finally, termination of further polymerization could be the result of a specific blockade (capping) of filament ends imposed after connecting IF to the plasma membrane skeleton (12).

This model, of course, which is mainly based on affinity considerations, could be influenced by other parameters such as the relative numbers of attachment sites for IFs expressed at a given developmental stage along the major membranes. It might also be modified if indeed various posttranslational modifications of IF subunits affect their functional properties. However, since the expression of ankyrin seems to be constitutive during erythropoesis and since the phosphorylation of vimentin does not directly relate with its polymerization state (31), we believe that the scenario described above constitutes the most likely assembly pathway, provided that we can extrapolate from in vitro data to in vivo operating principles.

We thank Dr. J. Aris for reading the manuscript and making useful suggestions. The help of Dr. C. R. Cantor (Columbia University) in the interpretation of quantitative data is greatly acknowledged.

This work was supported by National Institutes of Health grant GM-27155 and is dedicated to Elias Blountzos.

Received for publication 17 September 1986, and in revised form 6 February 1987.

References

1. Aebi, U., W. E. Fowler, P. Rew, and T. T. Sun. 1983. The fibrillar substructure of keratin filaments unravelled. *J. Cell Biol.* 97:1131–1143.
2. Beam, K. G., S. L. Alper, G. E. Palade, and P. Greengard. 1979. Hormonally regulated phosphoprotein of turkey erythrocytes. Localization to plasma membranes. *J. Cell Biol.* 83:1–15.
3. Blikstad, I., and E. Lazarides. 1983. Vimentin filaments are assembled from a soluble precursor in avian erythroid cells. *J. Cell Biol.* 96:1803–1808.

4. Bruns, G. A. P., and V. M. Ingram. 1973. The erythroid cells and haemoglobins of the chick embryo. *Philos. Trans. R. Soc. Lond. B Biol. Sci.* 266:225–305.
5. Ceriotti, G. 1952. A microchemical determination of desoxyribonucleic acid. *J. Biol. Chem.* 198:297–303.
6. Fenner, C., R. R. Traut, D. T. Mason, and J. Wilkman-Coffelt. 1975. Quantification of Coomassie-blue stained proteins in polyacrylamide gels based on analysis of eluted dyes. *Anal. Biochem.* 63:595–602.
7. Franke, W. W. 1971. Relationship of nuclear membranes with filaments and microtubules. *Protoplasma.* 73:263–292.
8. Fraser, R. D. B., T. P. MacRae, E. Suzuki, D. A. D. Parry, A. C. Trajstman, and I. Lukas. 1985. Intermediate filament structure 2. Molecular interactions in the filament. *Int. Rev. Biol. Macromol.* 7:258–274.
9. Geisler, N., E. Kaufmann, and K. Weber. 1982. Protein chemical characterization of three structurally distinct domains along the protofilament unit of desmin 10 nm filaments. *Cell.* 30:277–286.
10. Geisler, N., E. Kaufmann, and K. Weber. 1985. Anti-parallel orientation of the two double-stranded coiled-coils in the tetrameric protofilament unit of intermediate filaments. *J. Mol. Biol.* 185:173–177.
11. Georgatos, S. D., and V. T. Marchesi. 1985. The binding of vimentin to human erythrocyte membranes: a model system for the study of intermediate filament–membrane interactions. *J. Cell. Biol.* 100:1955–1961.
12. Georgatos, S. D., D. C. Weaver, and V. T. Marchesi. 1985. Site-specificity in vimentin-membrane interactions: intermediate filament subunits associate with the plasma membrane via their head domains. *J. Cell Biol.* 100:1962–1967.
13. Georgatos, S. D. 1985. Molecular interactions between vimentin and the human erythrocyte membrane. Ph.D. Thesis. Yale University, New Haven, CT. 95 pp.
14. Granger, B. L., and E. Lazarides. 1982. Structural associations of synemin and vimentin in avian erythrocytes revealed by immunoelectron microscopy. *Cell.* 30:263–275.
15. Granger, B. L., E. A. Repasky, and E. Lazarides. 1982. Synemin and vimentin are components of intermediate filaments in avian erythrocytes. *J. Cell Biol.* 92:299–312.
16. Granger, B. L., and E. Lazarides. 1984. Membrane-skeletal protein 4.1 of avian erythrocytes is composed of multiple variants that exhibit tissue-specific expression. *Cell.* 37:595–607.
17. Hill, A. V. 1910. The possible effects of the aggregation of the molecules of hemoglobin on its dissociation curves. *J. Physiol. (Lond.).* 40:iv.
18. Jackson, R. C. 1976. Polypeptides of the nuclear envelope. *Biochemistry.* 15:5641–5651.
19. Kaufmann, E., K. Weber, and N. Geisler. 1985. Intermediate filament forming ability of desmin derivatives lacking either the aminoterminal 67 or the carboxyterminal 27 residues. *J. Mol. Biol.* 185:733–742.
20. Krohne, G., E. Debus, M. Osborn, K. Weber, and W. W. Franke. 1984. A monoclonal antibody against nuclear lamina proteins reveals cell-type-specificity in *Xenopus laeris*. *Exp. Cell Res.* 150:47–59.
21. Laemmli, U. K. 1970. Cleavage of structural proteins during the assembly of the heads of bacteriophage T_4. *Nature (Lond.).* 227:680–685.
22. Lazarides, E. 1984. Assembly and morphogenesis of the avian erythrocyte cytoskeleton. *In* Molecular Biology of the Cytoskeleton. G. G. Borisy, D. W. Cleaveland, and D. B. Murphy, editors. Cold Spring Harbor Laboratory, Cold Spring Harbor, NY.
23. Lowry, O. H., N. T. Rosebrough, A. L. Farr, and R. J. Randall. 1951. Protein measurement with the Folin-phenol reagent. *J. Biol. Chem.* 143: 265–275.
24. Nelson, W. J., and E. Lazarides. 1984. Goblin (ankyrin) in striated muscle: identification of the potential membrane receptor for erythroid spectrin in muscle cells. *Proc. Natl. Acad. Sci. USA.* 81:3292–3296.
25. Nelson, W. J., and P. Traub. 1983. Proteolysis of vimentin and desmin by a Ca^{2+}-activated proteinase specific for these intermediate filament proteins. *Mol. Cell. Biol.* 3:1146–1156.
26. Quax-Jenken, U., W. J. Quax, and H. Bloemendal. 1983. Primary and secondary structure of hamster vimentin predicted from the nucleotide sequence. *Proc. Natl. Acad. Sci. USA.* 80:3548–3552.
27. Ramaekers, F. C. S., I. Dunia, H. T. Dodemont, E. L. Bennedetti, and H. Bloemendal. 1982. Lenticular intermediate-sized filaments: biosynthesis and interaction with the plasma membrane. *Proc. Natl. Acad. Sci. USA.* 79:3208–3212.
28. Rueger, D. C., J. S. Huston, D. Dahl, and A. Bignami. 1979. Formation of 100 Å filaments from purified glial fibrillary acidic protein *in vitro*. *J. Mol. Biol.* 135:53–68.
29. Scatchard, G. 1949. The interaction of proteins with small molecules and ions. *Ann. NY Acad. Sci.* 51:660–672.
30. Shelton, K. R., C. S. Cobbs, J. T. Povlishock, and R. K. Burkat. 1976. Nuclear envelope fraction proteins: isolation and comparison with the nuclear protein of avian erythrocytes. *Arch. Biochem. Biophys.* 174:177–186.
31. Soellner, P., R. A. Quinlan, and W. W. Franke. 1985. Identification of a distinct soluble subunit of an intermediate filament protein: tetrameric vimentin from living cells. *Proc. Natl. Acad. Sci. USA.* 82:7929–7933.
32. Traub, P., and C. Vorgias. 1983. Involvement of the N-terminal peptide of vimentin in the formation of intermediate filaments. *J. Cell. Sci.* 63: 43–67.
33. Traub, P., G. Perides, H. Schimmel, and A. Scherbarth. 1986. Interaction *in vitro* of non-epithelial intermediate filaments with total cellular lipids, individual phospholipids and a phospholipid mixture. *J. Biol. Chem.* 261:10558–10568.
34. Wang, E. 1985. Intermediate filament associated proteins. *Ann. NY Acad. Sci.* 455:32–56.
35. Weber, K., and N. Geisler. 1985. Intermediate filaments: structural conservation and divergence. *Ann. NY Acad. Sci.* 455:126–143.
36. Woodcock, C. L. F. 1980. Nucleus-associated intermediate filaments from chicken erythrocytes. *J. Cell Biol.* 85:881–889.
37. Zackroff, R. V., and R. D. Goldman. 1979. *In vitro* assembly of intermediate filaments from BHK-21 cells. *Proc. Natl. Acad. Sci. USA.* 76:6226–6230.
38. Zehner, Z. E., and B. M. Patterson. 1985. The chicken vimentin gene. *Ann. NY Acad. Sci.* 455:89–94.